CHAPTER 3

BACKGROUND OF LIDAR

3.1 Introduction

Lidar or LIght Detection And Ranging is an instrument to observe atmospheric particle such as molecule of gas, aerosol, and cloud particle by remote sensing technique.

3.2 Lidar Principal

The operating principle of lidar is analogous to pulse microwave radar, except that lidar uses optical technique rather than microwave technique. A typical lidar system employs a pulse laser source such as Q-switch ruby, neodymium doped glass (Nd:YAG) to transmit light pulse into the atmosphere. An optical telescope mounted adjacent to the laser is used to detect backscattered echoes from scatterers in the path of the transmitted pulses. In contrast to radar, lidar generally uses separate transmitting and receiving optic, thereby yielding a non coaxial system with parallax. The light received by the telescope is focused onto a photo-detector such as photomultiplier, which yields an electronic signal proportional to the received light flux. The transient detector response is sampled and digitized. In order to improve signal to noise ratio, signals are multiplied in averaged over ten to thousands times of incoming pulses.

3.2.1 Lidar Equation

Following the radar practice, the lidar response may be quantitatively interpreted in terms of lidar equation. The instantaneous received power, $P(z)$, of backscattering at height z, assuming only single scattering and a vertically pointing lidar, may be expressed in the form,

$$P(z) = P_oY(z)[(ct_p)/2]\,(A_R/z^2)\beta(z)T^2(z) \qquad (1)$$

where P_o = transmitted peak power

$Y(z)$ = geometry factor for overlap of transmitter/receiver beam path

ct_p = transmitted pulse length; pulse duration t_p times speed of light c

A_R/z^2 = solid angle (sr) subtended by receiver aperture A_R at range z

$\beta(z)$ = unit of volume backscattering coefficient ($m^{-1}sr^{-1}$) of the atmosphere at range z

$T^2(z)$ = round-trip transmittance and from range z.

The attenuation factor T(z) follows the exponential law of attenuation, i.e. Beer-Lambert law. It is related to the optical depth or integrated extinction by

$$T(z) = e^{-\tau(z)}$$

or

$$T(z) = e^{-\int \sigma(z')dz'}$$

where $\tau(z)$ = the atmospheric optical depth through height z

$\sigma(z')$ = the atmospheric unit volume extinction coefficient (m^{-1}) at any intervening height z' between 0 and z.

Photodetection and post-detection amplification of the received power yields the lidar response output signal V(z), proportional to P(z). For ranges beyond complete overlap of the transmitter receiver beam paths, the working form of lidar becomes

$$V(z) = \frac{CE_o(z)\beta(z)T^2(z)}{z^2} \qquad (2)$$

The constituents in the atmosphere that interact transmitted lidar pulse and backscatter are compose of air molecule of specific gas and aerosol particles. Scattering of light by molecules is weak because of their relatively small size. It is called as Raleigh scattering that varies inversely with the fourth power of wavelength of the incident radiation. On the other hand, scattering and diffraction of light by atmospheric aerosol particles are relatively strong generally approximated as Mie scattering. While molecular scattering varies in proportion to the atmospheric molecular density at a given lidar wavelength, aerosol scattering varies in a complicated manner depending on size distribution and refraction induced by aerosol particles. Aerosol properties vary significantly from place to place and one time to another, thereby making it virtually impossible to accurately predict aerosol scattering contribution to a given lidar signal. In contrast, the molecular scattering contribution can be predicted rather accurately using standard atmospheric information or by using sounding data for the time and place of interest.

The molecule and aerosol scattering contributions may be treated by superposition so that $\beta(z)$ may be express as

$$\beta(z) = \beta_R(z) + \beta_a(z) \qquad (3)$$

where $\beta_R(z)$ and $\beta_a(z)$ are the Rayleigh (molecular) and aerosol backscattering coefficients, respectively.

Similarly, $\sigma(z)$ may be expressed as

$$\sigma(z) = \sigma_R(z) + \sigma_a(z)$$

Then

$$T(z) = \exp\left[-2\int[\sigma_R(z') + \sigma_a(z')]dz'\right] \qquad (4)$$

where σ_R and σ_a are the Rayleigh (molecule) and aerosol attenuated coefficients, respectively. For range beyond complete overlap of the transmitter receiver beam path, the working form of lidar becomes

$$V(z) = \frac{CE_o[\beta_R(z) - \beta_a(z)] \exp[-2\int\{\sigma_R(z') + \sigma_a(z')\}dz']}{z^2} \quad (5)$$

The Rayleigh term can be eliminated by the Rayleigh scattering law and surface meteorological data. The problem to solve lidar equation is that aerosols term contain two unknowns. Various solution methods have been developed to overcome these difficulties.

3.2.2 Lidar Equation Solution

The simplest method to solve the problem of lidar equation is to assume the atmosphere is homogeneous. In this sense, the total backscattering and extinction coefficient are constant over lidar signal path, the total extinction coefficient may be retrieved by slop method.

The range-squared and energy normalized lidar signal as expressed by

$$X(z) = \frac{z^2V(z)}{E_o} = C\beta(z)\, e^{-2\int\sigma(z')dz} \quad (6)$$

In this research, we used Fernald's method to solve the problem from lidar data. Fernald et al., 1972 suggested that the lidar equation solution is based on the assumption that the aerosol extinction-to-backscatter ratio, σ_a/β_a, expressed as S, is constant along lidar signal path. With this constraint, the normalized lidar equation reduces into simple, easily solvable differential equation given by

$$\frac{dT_a^2(z)}{dz} = \frac{-2SX(z)}{C} \quad (7)$$

for the one-scatterer (i.e., dominant aerosol scattering)

$$\frac{dT_a^2(z)}{dz} - 2S\beta_R(z)T_a^2(z) = \frac{-2SX(z)}{CT_R^2(z)} \qquad (8)$$

for the more general two-scatterer- (molecular and aerosol scattering) case Fernald solved the (6) for $T^2(z)$ over an interval z = 0 to z, as given by

$$T^2(z) = 1 - 2S\int X(z')dz'/C \qquad (9)$$

and for the (7) is given by

$$T_a^2(z) = T_R(z)^{-3S/4\pi}\{1 - 2S\int X(z')T_R(z')^{[(3S/4\pi) - 2]}dz'\} \qquad (10)$$

for the two-scatterer-case σ_R/β_R = $8\pi/3$. Thus with given S, $T^2(z)$ or $T_a^2(z)$ can be determined, and $\beta(z)$ or $\beta_a(z)$ may be retrieved from the normalized lidar equation by

$$\beta(z) = X(z)/T^2(z)$$

and

$$\beta_a(z) = [X(z)/C\ T_a^2(z)] - \beta_R(z) \qquad (11)$$

where C, $\beta_R(z)$, and $T_R^2(z)$ are assumed. Alternately, if $T^2(z)$ or $T_a^2(z)$ are known at only one height $z = z_1$, S can be obtain from (6) and (8) which, for the one type of scatter case, yields

$$S = 2C\ [1 - T^2(z_1)]/\int X(z)dz \qquad (12)$$

Once S is known, $T^2(z)$ or $T_a^2(z)$ and $\beta(z)$ or $\beta_a(z)$ may be retrieved for any z less than z_1 as outlined above. The retrieval of $\beta(z)$ or $\beta_a(z)$ also provides $\sigma(z)$ and $\sigma_a(z)$ through the relation $\sigma_a(z) = S\beta_a(z)$.

3.3 Lidar observation at the Observatory for Atmospheric Radiation Research at Sri Samrong, Sukhothai

3.3.1 Micro Pulse Lidar or MPL

Micro Pulse Lidar or MPL has been installed at the Observatory since July 1997 by Professor Nobuo Takeuchi of Chiba University. MPL set is composed of a laser power supply section, a scaler and a controller section, a MPL telescope and a personnel computer (PC) (Figure 3.1). Diode laser power from the laser power supply section is feeded to a laser source inside the MPS telescope via fiber optic cable. Inside the laser source are neodymium-doped yttrium fluoride (Nd:YLF) which is a laser head and Q-switched, a transmitted pulse. Laser source generates 532.5 nm green light which is directed to the telescope through many optical components such as beam splitter to directed laser beam to the telescope and also directed backscattering signal to detector. The pulse duration of laser beam is approximately 10 ns. The pulse repetition rate can be varied from 1 Hz to 10 kHz with the remote control of the laser source. The returned green light from backscattering of atmospheric particle to the telescope is directed to the photon counting detector through polarizing beam splitter. The photon counting detector generates Total Tracking Laser (TTL) pulses of duration about 10 ns in proportion to the number of backscattering photons. The detector pulses are counted, stored by scaller and controller. The stored number of counts are averaged by the PC and displayed on screen.

Since MPL was not fully developed device, lidar observation has been frequently interrupted (Figure 3.2). Moreover, MPL data frequently showed strong backscattering signal at about 1 km (Figure 3.3). We found the false signal came from Iris, a small metal cycle with small hole at center, with diameter about 532 nanometer, was insufficient for noise reduction. After iris hole was expanded, the geometry factor of field-of-view increased. It, however, turned out high laser energy came from laser source. In order to prevent this problem, we moved laser source to outside of MPL telescope (Figure 3.1A). After the modification, laser beam expansion became very small (Figure 3.1B). It makes alignment of laser beam difficult. In addition, laser expander durable for laser from laser source was limited only 3 months. Finally, we abandon to use MPL.

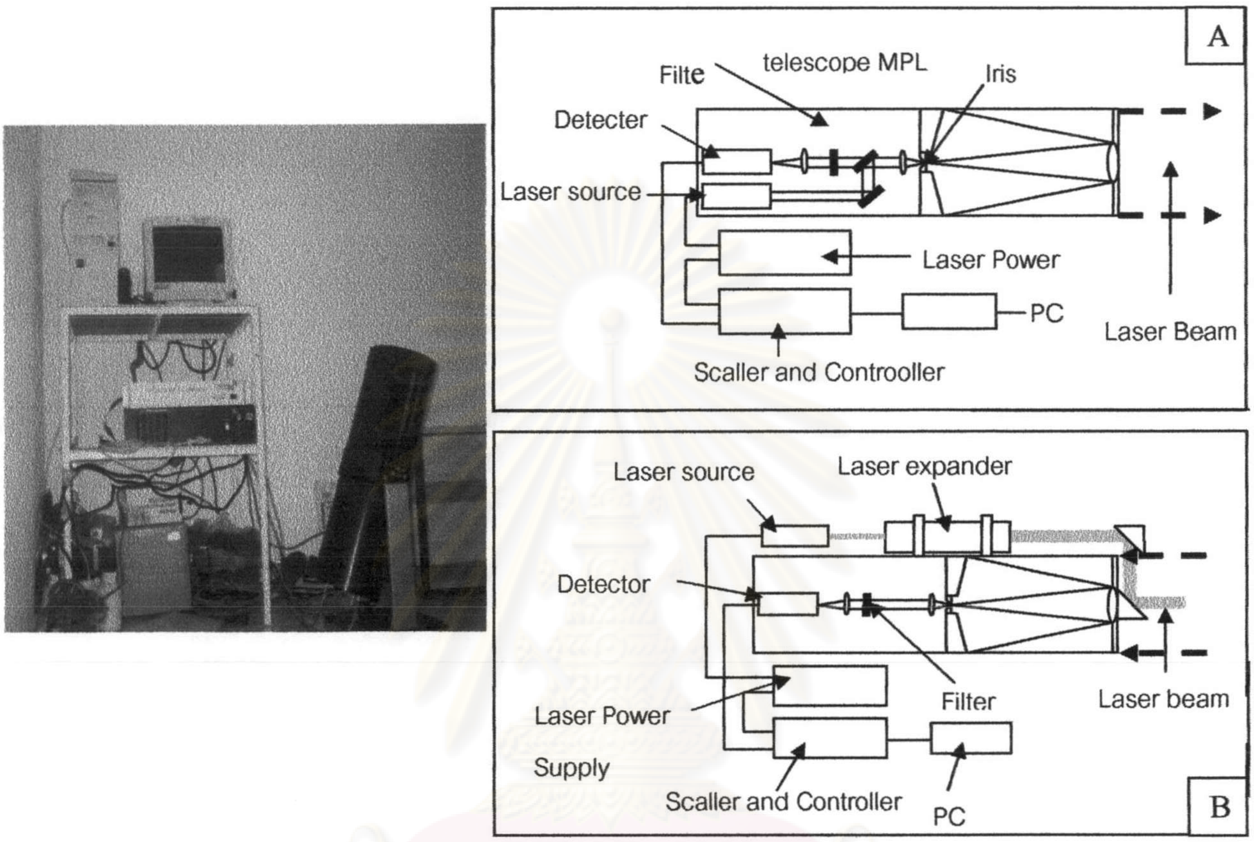

Figure 3.1 Micro Pulse Lidar, schematic A before modification and schematic B after modification

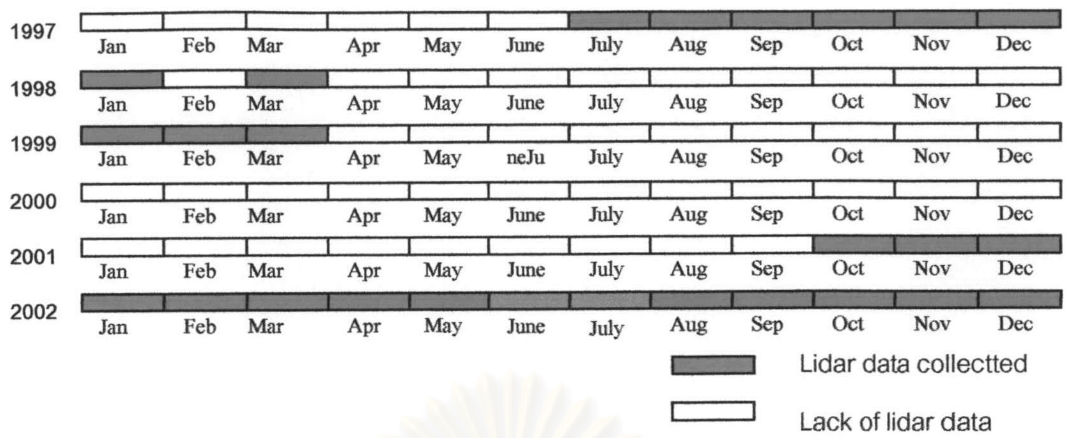

Figure 3.2 Lidar data collection from1997 to 2002

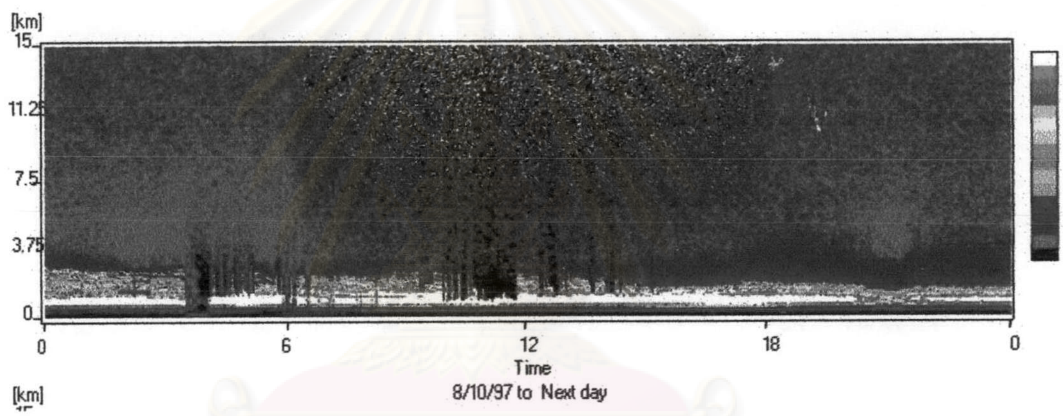

Figure 3.3 MPL data collected at 8 October 1997. Vertical axis is height (km), horizontal axis is time, and colors represent backscattering intensity. White expresses the highest backscattering intensity and black represent the lowest backscattering intensity. The white line is fault signal from Iris hole expansion.

3.3.2 Mie Scattering Lidar

Mie Scattering Lidar was installed at the Observatory in October 2001 by Dr. Nobuo Sugimoto. Mie Scattering Lidar system consists of a lidar head, a laser power supply, a digital oscilloscope, a data acquisition computer (Figure 3.4). The lidar employs flashlamp pumped Nd:YAG laser (532 nm, second harmonic and 1064 nm, first harmonic). Laser beam is transmitted after collimated with a beam expander. The scattered light is received with 20 cm Schmidt Cassegrain telescope. The received light is collimated and directed to the polarizer to separate parallel and perpendicular components. Separated polarize components are detected with the two photomultiplier tubes (PMTs). With the dual polarization measurement function, sphericity of scatterer can be estimateed (Figure 3.5). Thus water cloud and ice cloud can be distinguished. Detected lidar signals are recorded with the digital oscilloscope and averaged, and then transferred to the data acquisition computer. The data are averaged further and stored on the hard disk. The response of photomultiplier is fast and high gain coupled with fairly good quantum efficiency and relatively low noise levels, even at or near room temperature. However, photomultipliers become very inefficient over wavelength 900 nm. Hence, in October 2002, Advance Photo Diode (ADP) of first harmonic with wavelength 1064 nm was installed by Dr. Nobuo Sugimoto.

$$\text{Depolarization ratio} = \frac{\text{perpendicular to polarizer backscattering signal}}{\text{parallel to polarizer backscattering signal}} \qquad (13)$$

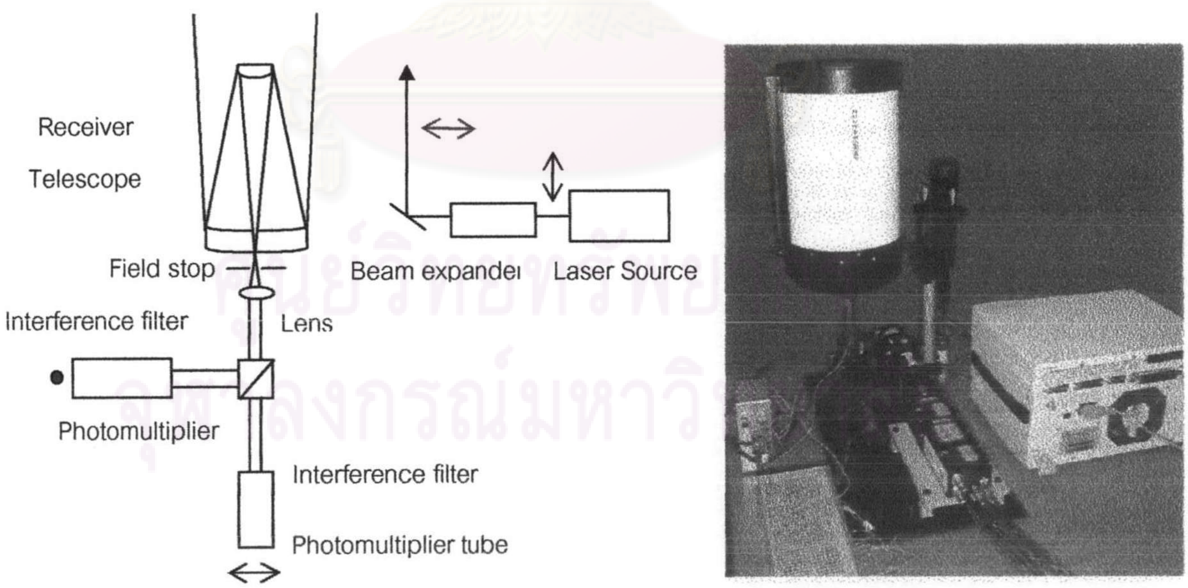

Figure 3.4 Mie Scattering Lidar

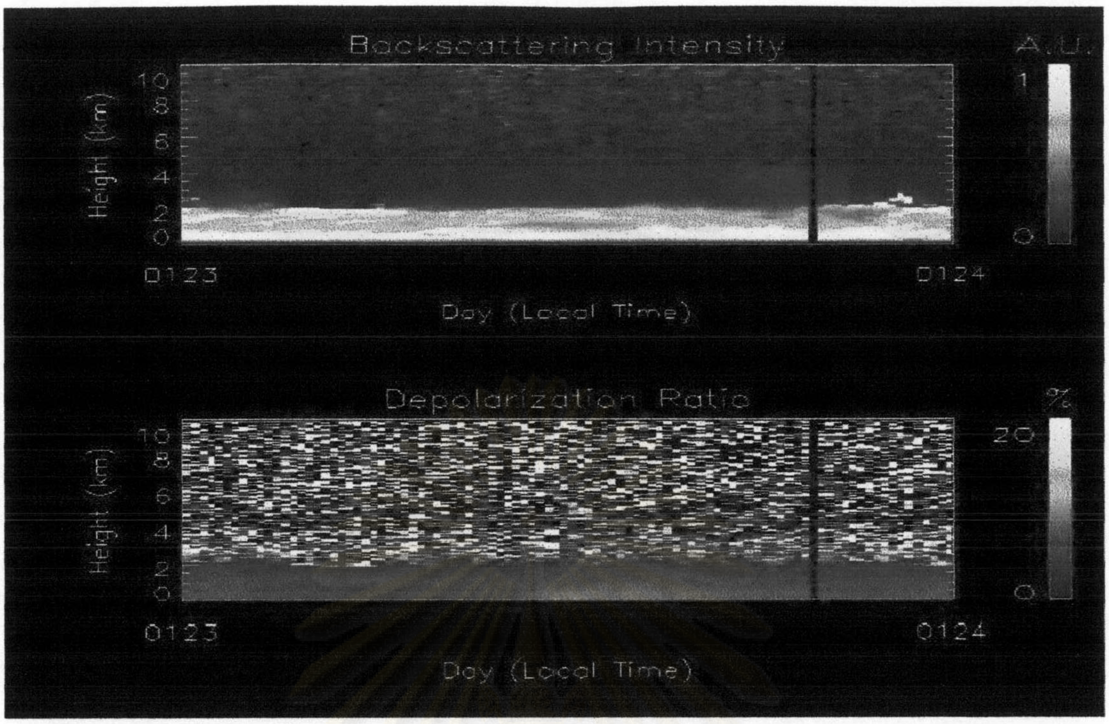

Figure 3.5 An example of Mie Scattering Lidar, Backscattering signal intensity data (Top), Depolarization ratio data (Down)

Parameter	(MPL)dar Micro Pulse Li	Mie Scattering Lidar
Laser Source	YLF:Nd	YAG:Nd
Wavelength	nm 532	nm 1064nm and 532
Energy	micro joule 5	mJ 30
Frequency	Hz 2500	pps 10
Telescope	Cassegrain	Cassegrain
Diameter	m 0.2	m 0.2
FOV	micro radian 100	m radian 1
Resolution	m 30	m 6

Table 3.1 Detail of Micro Pulse Lidar and Mie Scattering Lidar specification

3.3.3 Lidar data analysis

Lidar data delete utilized in this research is composed of backscattering lidar signal intensity or backscattering intensity, depolarization ratio and aerosol extinction coefficient data. The backscattering intensity is lidar signal intensity that is scattered by atmospheric particle and returned back to detector (Figure 3.6). Depolarization ratio data is evaluated from perpendicular and parallel backscattering signal ratio (Figure 3.6). Aerosol extinction coefficient is calculated by attenuated lidar signal in the atmosphere (Figure 3.7).

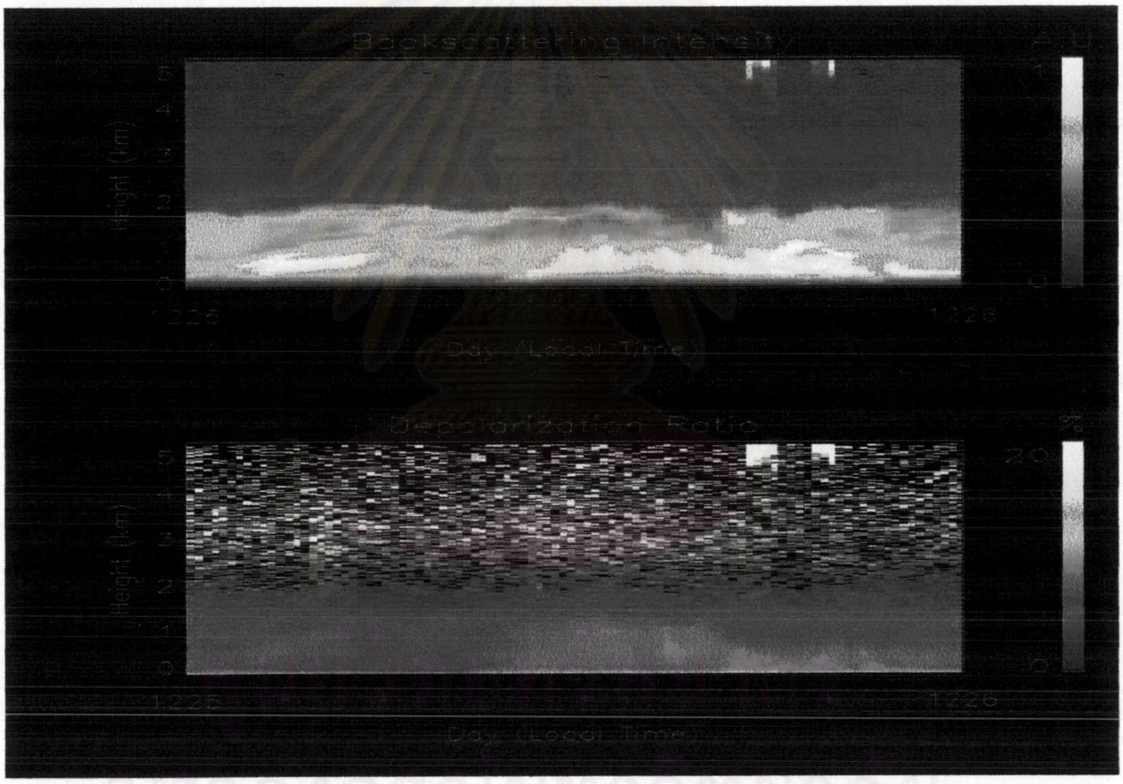

Figure 3.6 Backscattering intensity (up) and depolarization ratio data (down) observed at 25th December 2001.

In Figure 3.6 for backscattering intensity and depolarization ratio data, vertical and horizontal axes are range and time, respectively. Color represent backscattering intensity and depolarization ratio as defined in a scale bar. For aerosol extinction coefficient data (Figure 3.7), vertical and horizontal axis represent range and aerosol extinction coefficient.

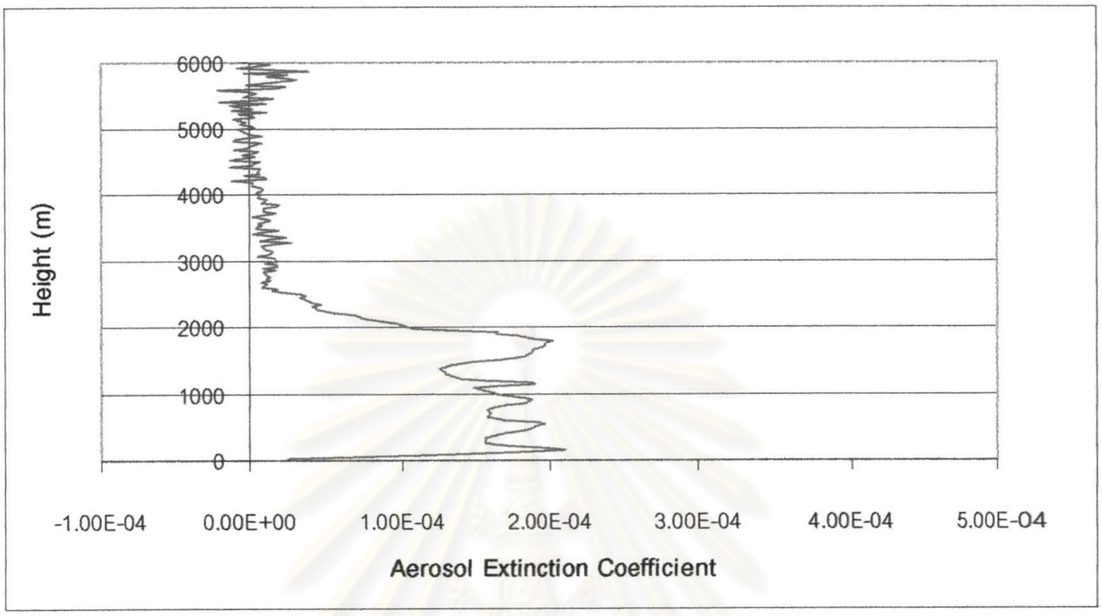

Figure 3.7 Aerosol backscattering coefficient data evaluated from backscattering intensity data that observed at 09:00 a.m., 23rd January 2002.

Laurent (1999) suggested backscattering lidar signal is proportional to the aerosol content of the atmosphere. Since the mixed layer is typically moister and has greater aerosol contents than free troposphere, backscattering of lidar signals are expected to be more intense. Thus, an ABL top height can be distinguished by top of high backscattering intensity and aerosol extinction coefficient layer for a dry season. On the other hand, a cloud base height is used to identify top of ABL in rainy season because the backscattering intensity is very low until could not ABL (Figure 3.8).

However, cloud base height had been used to identify top of ABL in rainy season because the backscattering intensity showed very low aerosol concentration until could not see ABL (Figure 3.8).

Laser is coherent wave therefore laser beam emit from laser source in the same plane. Backscattering signal from spherical scatterer introduce low depolarization ratio, whereas the backscattering signal from non spherical scatterer introduce high depolarization ratio. Depolarization ratio had been calculated by operating computer follow (13).

Figure 3.8 Backscattering intensity (up) and depolarization ratio data (down) observed at 9th September 2001, in rainy season.